Akt and mTOR pathways differentially regulate the development of natural and inducible T_H17 cells

Jiyeon S Kim, Tammarah Sklarz, Lauren Banks, Mercy Gohil, Adam T Waickman, Nicolas Skuli, Bryan L Krock, Chong T Luo, Weihong Hu, Kristin N Pollizzi, Ming O Li, Jeffrey C Rathmell, Morris J Birnbaum, Jonathan D Powell, Martha S Jordan &

Gary A Koretzky

Supplementary Figures 1 – 10

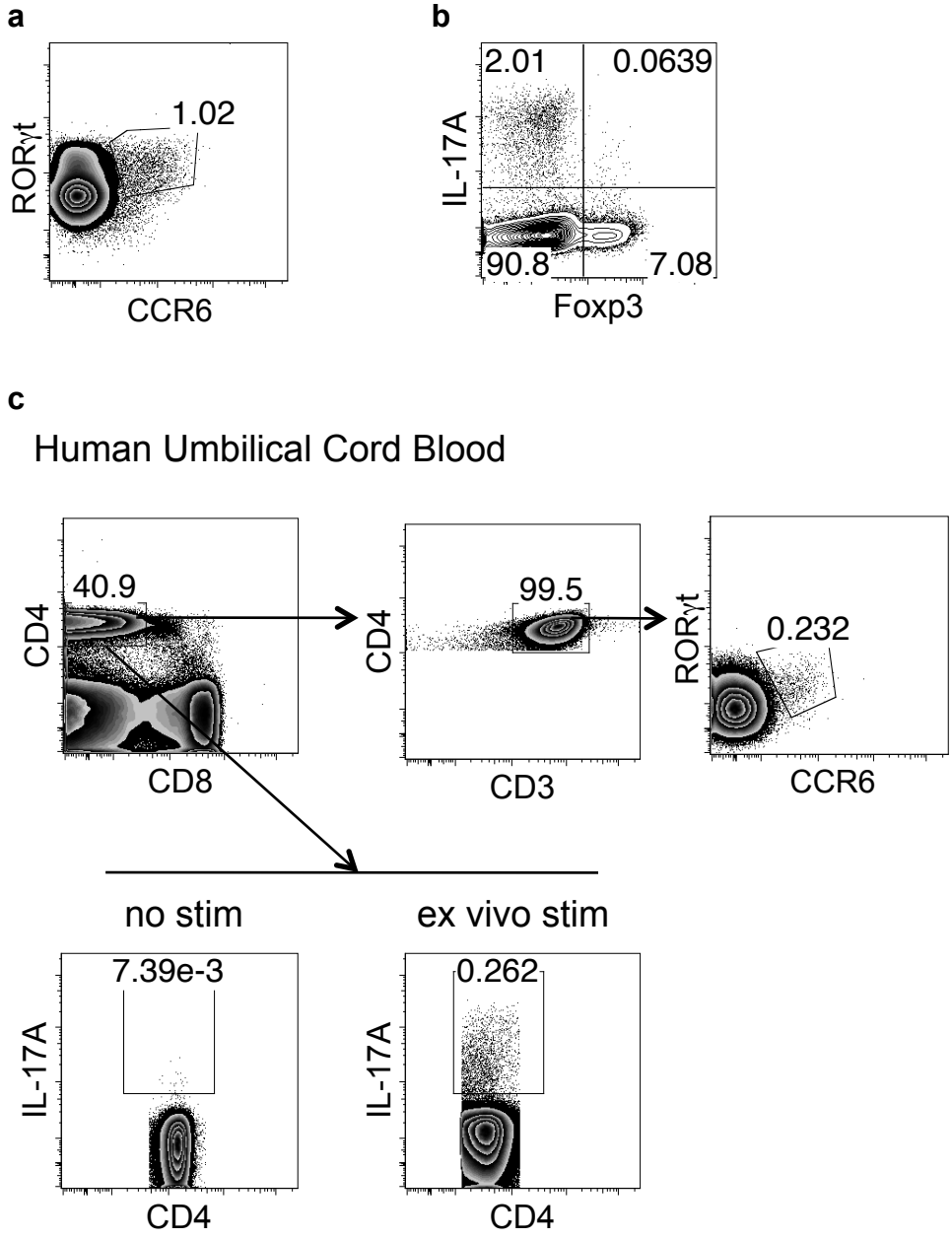

Supplementary Figure 1. nT_H17 cells are present in human thymus and umbilical cord blood. (a) Thymocytes from 18-19-week human fetal thymi were stained for RORγt and CCR6 expression. Flow plot are gated on $CD4^{SP}$ cells. **(b)** Thymocytes from 18-19 week human fetal thymi were stained for IL-17 and Foxp3 following *ex vivo* stimulation for 5 h with PMA/ionomycin and brefeldin A. Flow plots are gated on $CD4^{SP}$ cells. **(c)** Cells from umbilical cord blood were isolated and stained for surface markers and intracellular expression of IL-17A upon *ex vivo* stimulation for 5 h with PMA/ionomycin and brefeldin A. Gating strategy as shown. Data are representative of at least three independent experiments. Numbers indicate percentages for the gated populations.

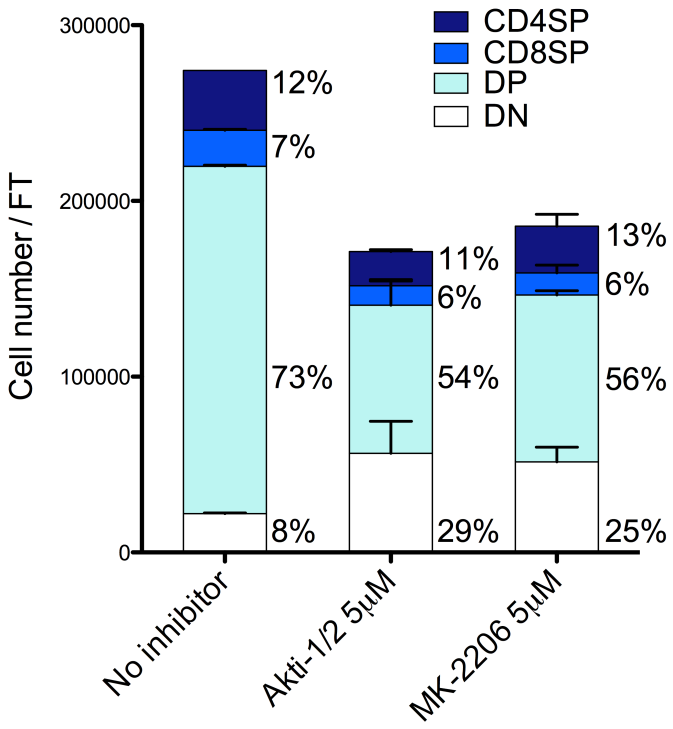

Supplementary Figure 2. Effect of Akt inhibitor treatment on thymocyte subsets in FTOC. Thymocytes from d7 of E15-initiated FTOC, cultured for the last 2 days in the presence of indicated concentrations of allosteric Akt inhibitors, were analyzed. Percentage of each thymocyte population is indicated. Data are pooled from two (MK-2206) and three (Akti-1/2) independent experiments (n = 4-5; mean ± SEM).

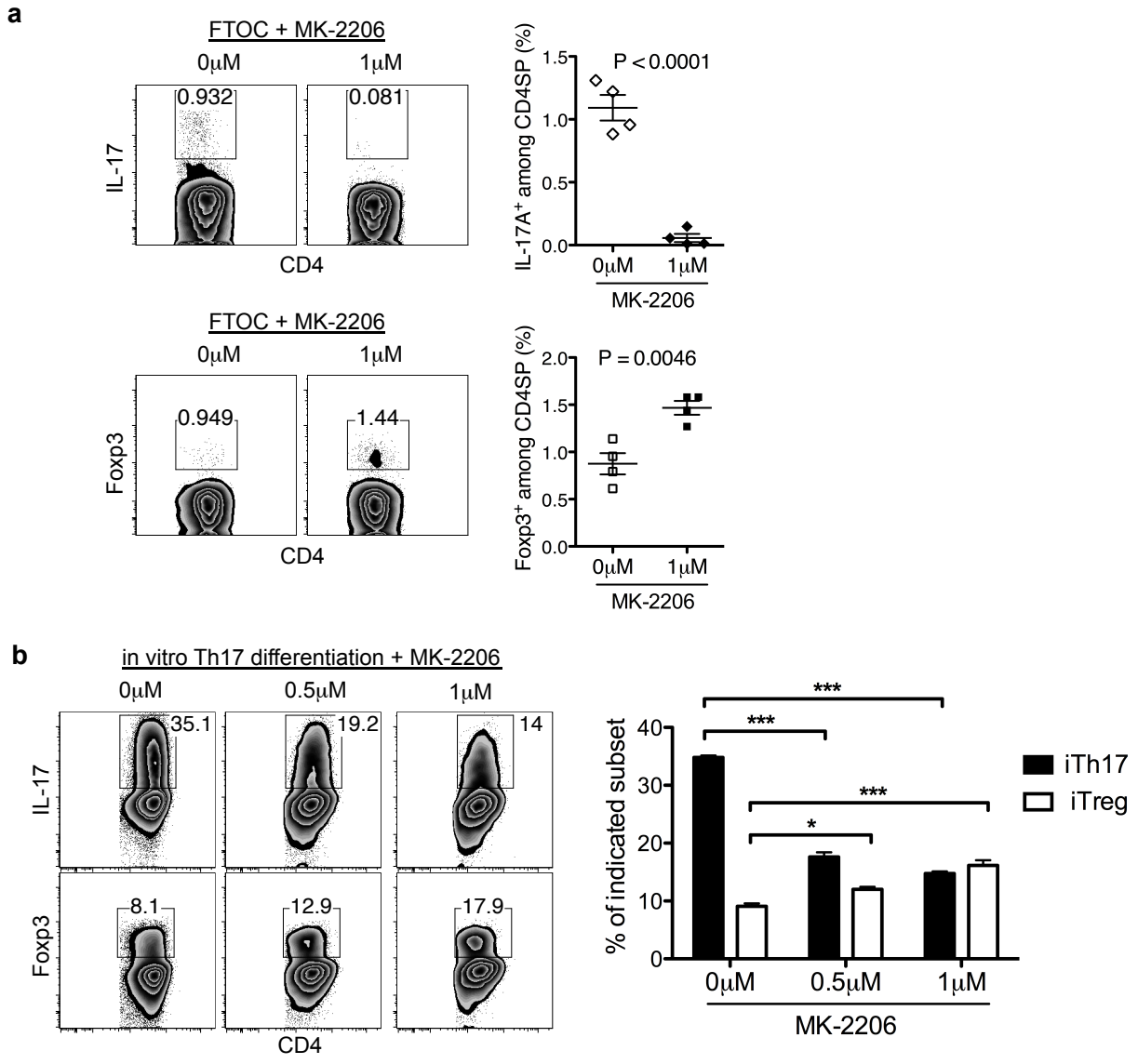

Supplementary Figure 3. Allosteric Akt inhibitor MK-2206 treatment impairs nT_H17 cell development in FTOC. (a) Cells from d7 of E15-initiated FTOC, cultured for the last 2 days in the presence of indicated concentrations of allosteric Akt inhibitor MK-2206, were stimulated with PMA/ionomycin and analyzed. Representative flow plots are gated on $CD4^{SP}TCR\beta^{+}TCR\gamma\delta^{-}$ cells. Graphs show either the percent of IL-17^{+} or $Foxp3^{+}$ cells among $CD4^{SP}$ cells pooled from two independent experiments (n = 4; mean ± SEM; P value from two-tailed Student's t-test). **(b)** IL-17 or Foxp3 expression is shown for WT naïve $CD4^{+}$ T cells activated for 18 h with anti-CD3 plus anti-CD28, followed by 36 h culture with iT_H17-polarizing condition in the presence of indicated concentrations of MK-2206, and 5 h re-stimulation with PMA/ionomycin with brefeldin A. Representative flow plots are shown. The graph shows pooled data from n = 3 per condition and bars and error bars represent mean ± SEM. *$P \leq 0.05$, ***P≤0.001 (one-way ANOVA followed by Dunnett's post-test with 0 μM as control group).

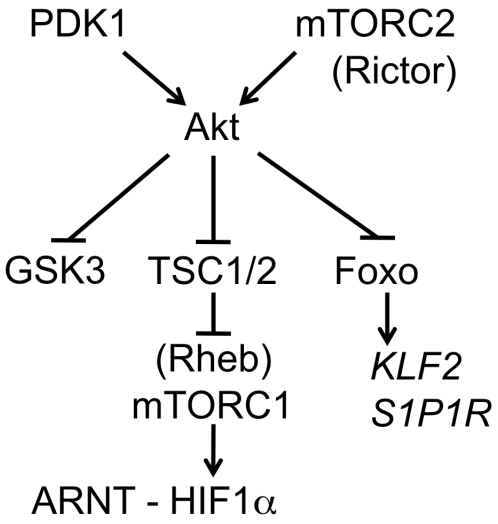

Supplementary Figure 4. Schematic of the Akt pathway.

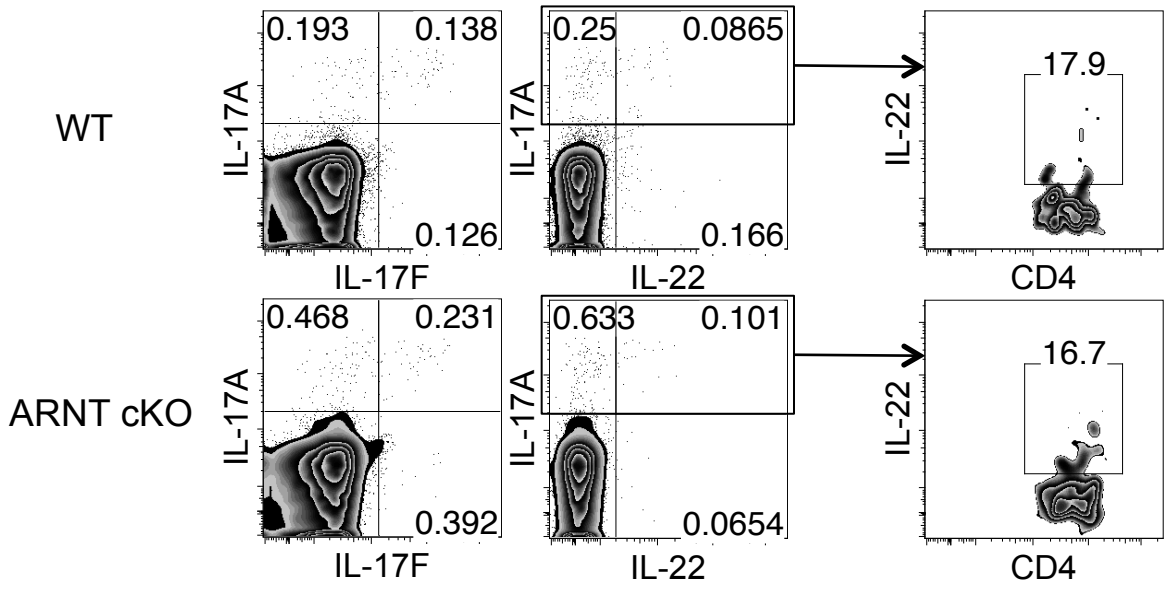

Supplementary Figure 5. IL-22 and IL-17F expression is intact in ARNT-deficient nT_H17 cells. IL-17F and IL-22 expression in thymocytes from WT and ARNT-cKO mice following *ex vivo* stimulation is shown. Representative flow plots are gated on $CD4^{SP}TCR\beta^{+}TCR\gamma\delta^{-}$ cells (first and second columns) or $IL\text{-}17A^{+}CD4^{SP}TCR\beta^{+}TCR\gamma\delta^{-}$ cells (third column). Data are from two independent experiments.

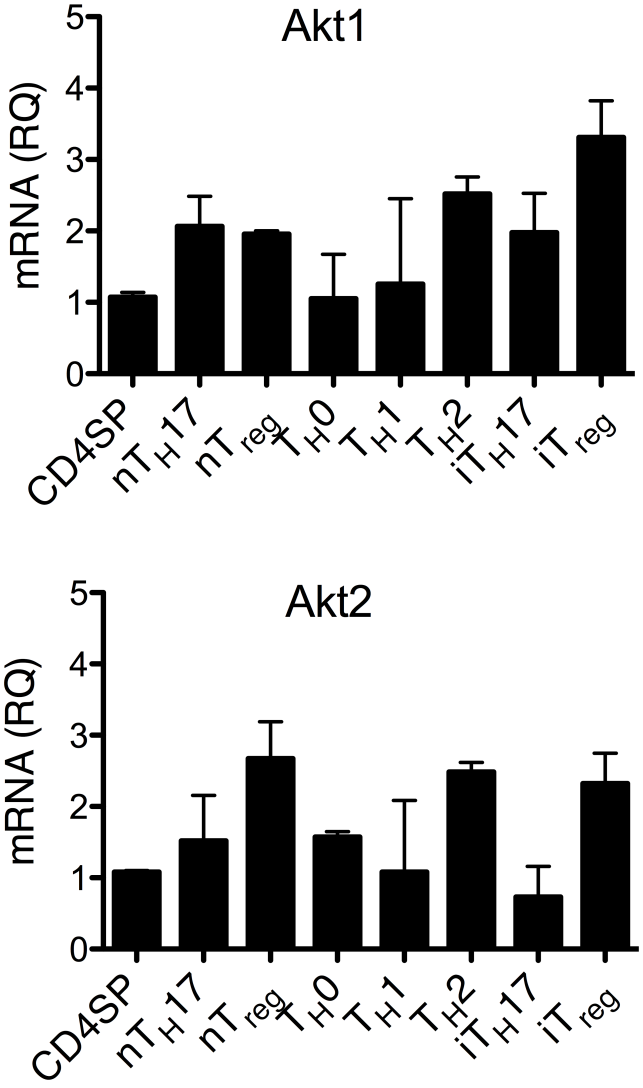

Supplementary Figure 6. mRNA expression of Akt1 and Akt2 in CD4$^+$ T cell subsets and thymocyte populations. Akt1 and Akt2 mRNA transcripts from either *in vitro* differentiated CD4$^+$ T cells (T_H0, T_H1, T_H2, iT_H17, iT_{reg}) or sorted WT thymocytes ($CD4^{SP}$, $CD4^+CD44^{lo}CCR6^-$; nT_H17, $CD4^+CD44^{hi}CCR6^+$; nT_{reg}, $CD4^+Foxp3^+$ from Foxp3-GFP reporter mice), relative to β-actin, was determined by real-time PCR. cDNA was generated from 3 independently sorted thymic populations or 2 independently generated T_H subsets. All samples were run in triplicate; bars and error bars represent mean ± SEM.

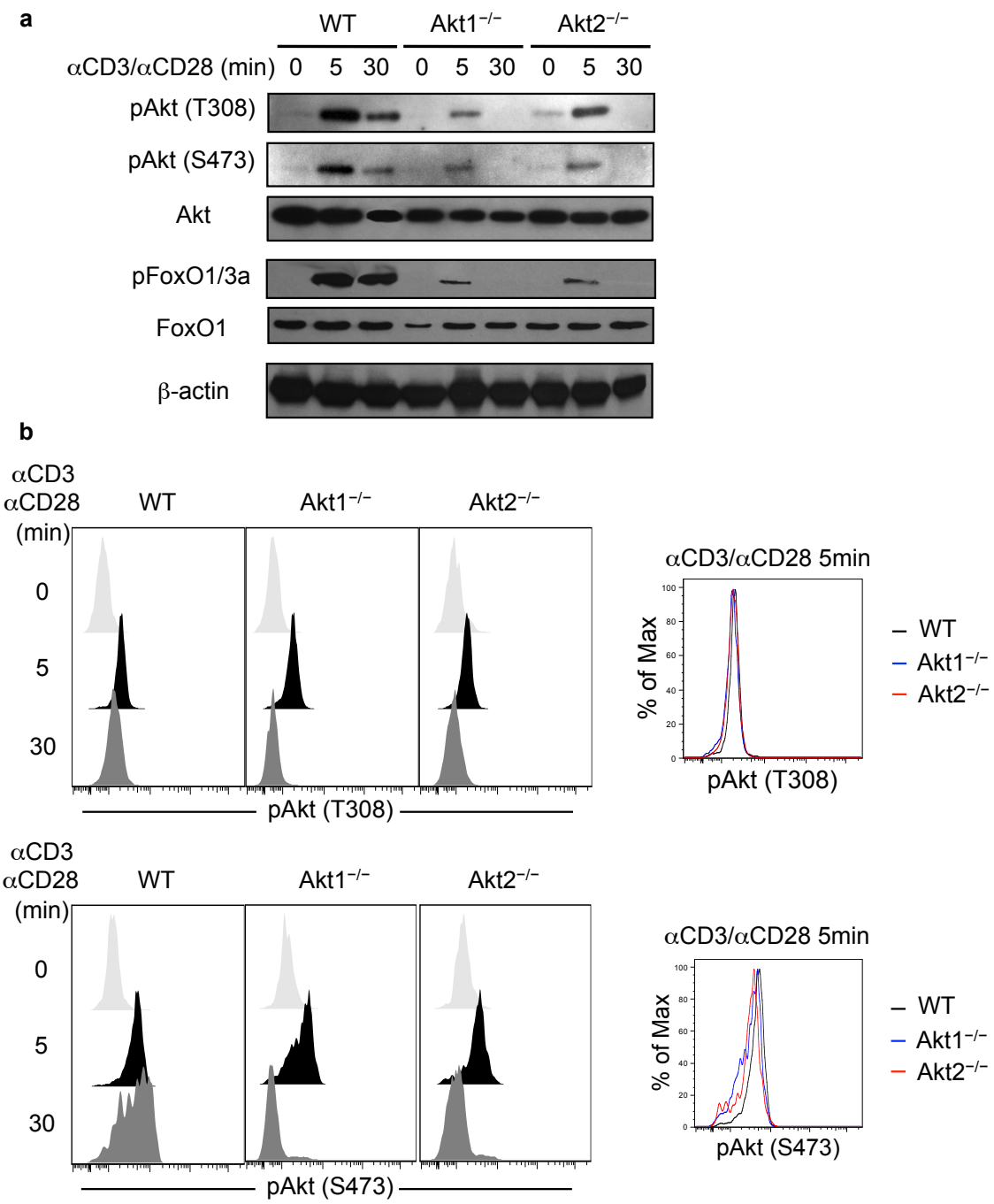

Supplementary Figure 7. Akt1 and Akt2 contribute equally to the pool of active Akt in CD4$^+$ T cells. (a) Immunoblot analysis of Akt activation, assessed by phosphorylation of p-Akt (T308) (n = 2), p-Akt (S473) (n = 1) and p-Foxo1/3a proteins (n = 2), in WT, *Akt1*$^{-/-}$, and *Akt2*$^{-/-}$ CD4$^+$ T cells stimulated for 5 min or 30 min with anti-CD3 and anti-CD28. **(b)** Phospho-flow analysis of Akt activation at indicated residue (T308 and S473) in WT, *Akt1*$^{-/-}$ and *Akt2*$^{-/-}$ CD4$^+$ T cells stimulated for 5 min or 30 min with anti-CD3 and anti-CD28. Data are representative of two independent experiments with n ≥ 5 per genotype.

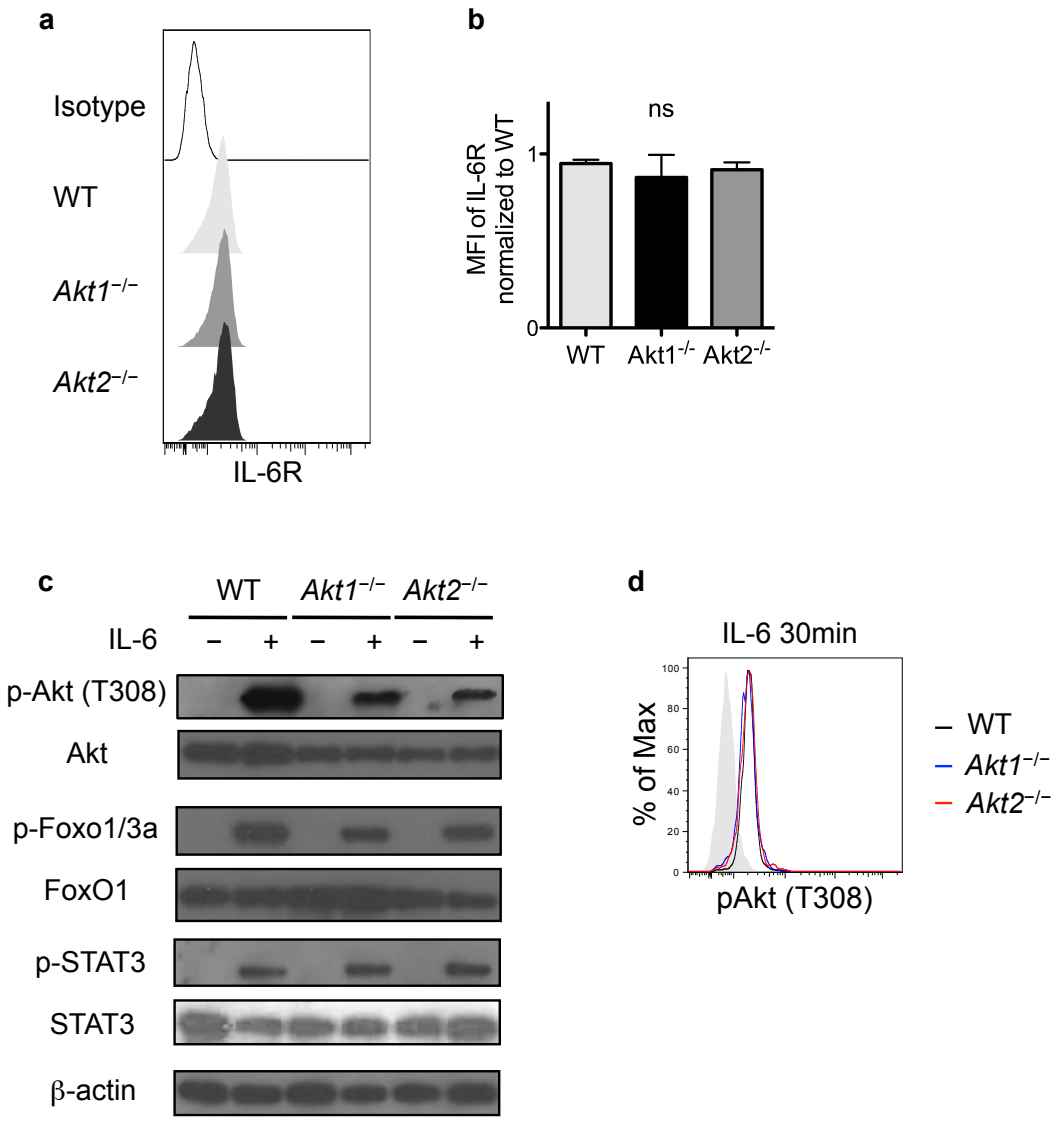

Supplementary Figure 8. IL-6 does not differentially activate Akt1 versus Akt2. (a) Expression of IL-6R (CD126) in WT, *Akt1*$^{-/-}$ and *Akt2*$^{-/-}$ CD4^{+} T cells analyzed by flow cytometry. Data are representative of two independent experiments (n ≥ 5 per genotype). **(b)** Expression of IL-6R in WT, *Akt1*$^{-/-}$ and *Akt2*$^{-/-}$ CD4^{+} T cells compared by mean fluorescence intensity (MFI). Graph shows pooled data from $n \geq 5$ mice per genotype and bars and error bars represent mean ± SEM. ns, not-significant (one-way ANOVA followed by Dunnett's post-test with WT as control group). **(c)** Immunoblot analysis of Akt activation, assessed by phosphorylation of Akt (p-Akt) and Foxo (p-Foxo1/3a) proteins, in WT, *Akt1*$^{-/-}$ and *Akt2*$^{-/-}$ CD4^{+} T cells stimulated with IL-6 for 30 min. Phosphorylation of STAT3 (p-STAT3) serves as positive control. Data are representative of two independent experiments. **(d)** Phospho-flow analysis of Akt activation in WT, *Akt1*$^{-/-}$ and *Akt2*$^{-/-}$ CD4^{+} T cells stimulated with IL-6 for 30 min. Shaded histogram represents unstimulated cells. Data are representative of two independent experiments with $n \geq 5$ per genotype.

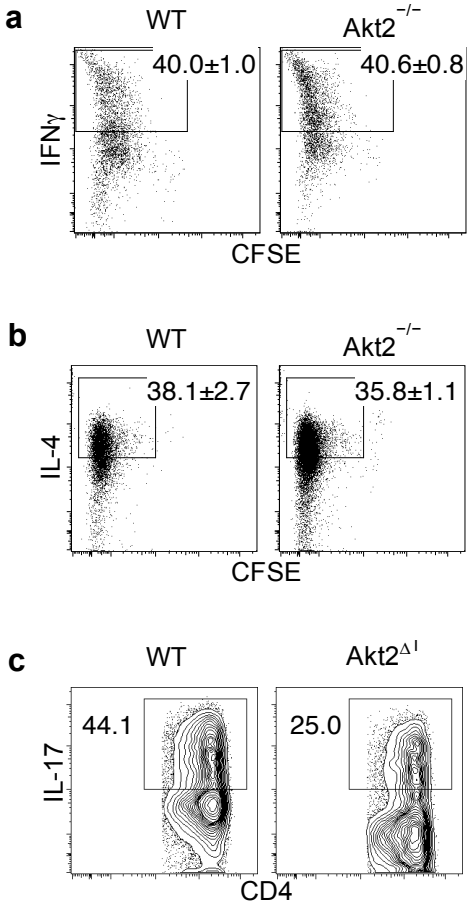

Supplementary Figure 9. T_H1 and T_H2 cell differentiation is intact in *Akt1*$^{-/-}$ and *Akt2*$^{-/-}$ CD4$^+$ T cells. (a) CFSE dilution and IFN-γ production is shown for WT and *Akt2*$^{-/-}$ CD4$^+$ T cells that were cultured with plate-bound anti-CD3 plus anti-CD28 in T_H1-polarizing condition for 4 days. **(b)** CFSE dilution and IL-4 production is shown for WT and *Akt2*$^{-/-}$ CD4+ T cells that were cultured with plate-bound anti-CD3 plus anti-CD28 in T_H2-polarizing condition for 4 days. **(c)** iT_H17 differentiation is defective in *Akt*$^{\Delta T}$ mice. IL-17 production in WT (*Akt*$^{fl/fl}$ CD4*cre*$^-$) and *Akt2*$^{\Delta T}$ CD4$^+$ T cells cultured with plate-bound anti-CD3 plus anti-CD28 in T_H17-polarizing condition for 3 days. Data are representative of at least two independent experiments (**a-c**).

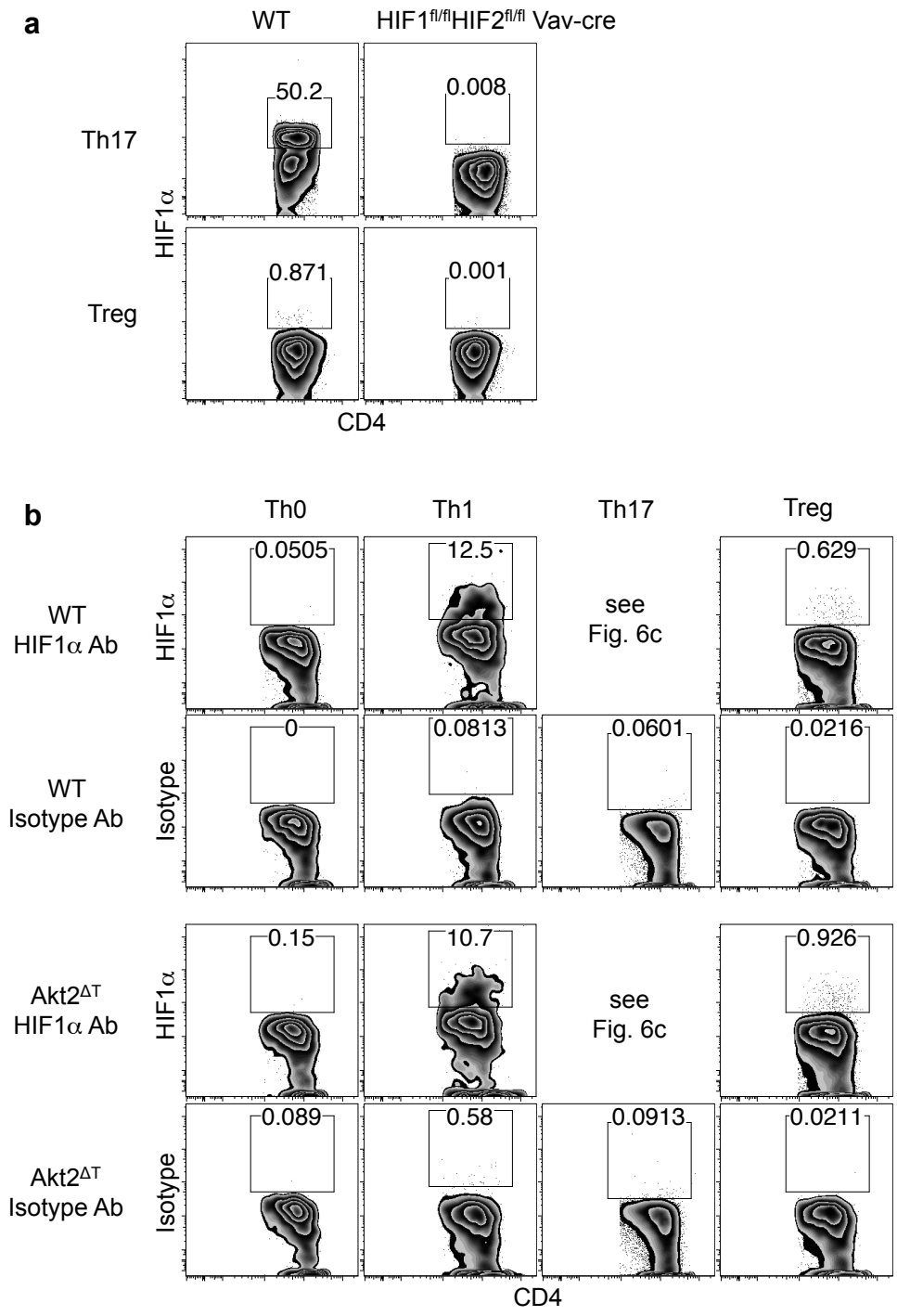

Supplementary Figure 10. Detection of intracellular HIF1α protein expression using flow cytometry. (a) HIF1α expression in WT and *Hif1a*$^{fl/fl}$*Hif2*$^{fl/fl}$ Vav-*cre* CD4^{+} T cells cultured with plate-bound anti-CD3 plus anti-CD28 in T_H17- or T_{reg}-polarizing condition; n = 1. **(b)** Intracellular staining using HIF1α or isotype antibody to assess HIF1α expression in WT and *Akt2*$^{fl/fl}$ Vav-*cre* (*Akt2*$^{\Delta T}$) CD4^{+} T cells cultured under T_H0, T_H1, T_H17 or T_{reg}-polarizing conditions. Representative plots from 2 independent experiments are shown.